# Hemodynamic investigation of intraluminal thrombus effect on the wall stress in a stented three-layered aortic aneurysm model under pulsatile flow

CrossMark

Mohammad Alagheband [a,b], Shahrokh Rahmani [a,b], Mansour Alizadeh [a,b], Alireza Karimi [a,b], Mahdi Navidbakhsh [a,b,*]

[a] School of Mechanical Engineering, Iran University of Science and Technology, Tehran 16846, Iran
[b] Tissue Engineering and Biological Systems Research Laboratory, School of Mechanical Engineering, Iran University of Science and Technology, Tehran 16846, Iran

**Abstract**    *Purpose:* Aortic aneurysms occurs when the wall stress exceeds the strength of the vascular tissue. Intraluminal Thrombus (ILT) may absorb tension and reduce the aortic aneurysm wall stress. The purpose of this study is to test the hypothesis that the presence and growth of ILT alters the wall stress in a stented aneurysm.
*Method:* A virtual stented aneurysm model with ILT is created to study the flow and wall dynamics by means of Fluid-Structure Interaction (FSI) analysis. Wall stresses are determined by two-dimensional axisymmetric finite element analysis. Calculations are performed as thrombus elastic modulus increased from 0.1 to 2 MPa and calculations are repeated as thrombus depth is increased in 10% increment until thrombus fills the entire aneurysm cavity.
*Results:* The blood flow velocity, pressure, and maximum wall stresses are compared to the aforementioned models. The maximum stress reduction of 46% occurs at the time of peak flow and 28% at the time of peak pressure when thrombus elastic modulus increases from 0.1 to 2 MPa. In addition, as the thrombus depth increased from 10% to 100 %, the wall stress at the time of peak flow and peak pressure decreased almost 25% and 20%.

* Corresponding author. School of Mechanical Engineering, Iran University of Science and Technology, Tehran 16846, Iran. Tel.: +98 21 77209027; fax: +98 21 73021585.
  *E-mail address:* mnavid@iust.ac.ir (M. Navidbakhsh).

*Conclusions:* The findings of this study may have implications not only for understanding the wall stress in ILT but also for providing more detailed information about aortic aneurysm with intraluminal thrombus.

## Introduction

Aneurysm is an irreversible bulge in weak parts of an artery which its occurrences in the abdominal aortic is more common than other parts of the vascular system. Abdominal Aortic Aneurysm (AAA) is a focal, balloon-like dilation of the terminal aortic segment that occurs gradually over a span of years.[1,2] This condition is growing in commonness in the aged people, with approximately 150,000 new cases being diagnosed every year.[3,4]

These aneurysms tend to enlarge over years but rupture abruptly when wall stress exceeds wall strength. These injuries are common in the aging population and, consequently, are increasingly responsible for morbidity and mortality.[5–9] Although the pathogenesis is still not well understood, there is an abundance of biological, clinical, histopathological, and mechanical data on AAAs, and there has been considerable improvement in the biomechanical modeling of these lesions.[10]

Excessive expansion of aneurysm eventually leads to its rupture, which is the thirteenth cause of mortality in the United States alone.[11] The traditional treatments for this problem include open surgery, cutting the damaged artery and its replacement with polyester graft. However, minimally invasive technique such as endovascular stent graft has been substituted nowadays.[12] Di Martino et al.[13] investigated a real three-dimensional abdominal aortic aneurysm and their results provided a quantitative local evaluation of the stresses due to local structural and fluid dynamic conditions. The structural and fluid dynamic conditions for aortic aneurysm were investigated by Liber et al.[14] They also considered thrombus and the interaction between thrombus and fluid and also investigated the influence of the stent filament size on the intra aneurysmal flow dynamics in a sidewall aneurysm model in vitro. Their result showed that the stenting procedure would significantly reduce the intra-aneurysmal vorticity and the mean circulation inside the aneurysm diminished reduced to less than 3% of its value before stenting.[15]

Wang et al. reconstructed realistic three-dimensional (3D) aortic aneurysm geometries, including both wall and ILT for four patients with ILT surface ratios that ranged from 0.29 to 0.72 and ILT volume ratios that ranged from 0.12 to 0.66. Their result showed that the peak wall stress reduces for all models with ILT include as compared with models with no ILT. Mower et al.[16] investigated a 2D axisymmetric finite element analysis to test the hypothesis that intraluminal thrombus can significantly reduce Abdominal Aortic Aneurysm (AAA) wall stress and their results indicated that the maximum stress reduction of 51% occurred when the thrombus with elastic modulus of 1.0 MPa filled the entire AAA cavity in comparison with a non-thrombus model. Furthermore, stresses were reduced by only 25% as modulus decreased to 0.2 MPa. Sun et al.[17] investigated the hemodynamic effect of stent struts on renal arteries in patients with abdominal aortic aneurysms. The stent wire thickness was simulated with a diameter of 0.4, 1.0, and 2.0 millimeters. In their results, the flow velocity was reduced by 20–30% in most of the situations when the stent struts thickness increased to 1.0 and 2.0 millimeters, respectively. A complex mechanical interaction between pulsatile blood flow and wall dynamics in the three-layered aortic arch model has been investigated by constructing three-dimensional model.[18] The variations of mechanical stress along the outer wall of the arch during the cardiac cycle have been also considered and variations of circumferential stress were found very similar to those of pressure.[18] The influence of arch aneurysm and wall stiffness on wall stress was considered in[18] and the results showed that the stresses are much higher at inflection points in the aneurysm model than in non-aneurysm model, and the stresses at media in stiffened wall are higher than in unstiffened wall.

In the present study, the effect of Young's modulus of thrombosis ($E_{th}$) and growth of thrombus depth on hemodynamic parameters and wall stress in a stented two-dimensional model of aneurysm is considered using Fluid-Structure Interaction (FSI) method. Other essential information and conditions to simulate this issue such as anatomy and geometry of model, mechanical properties of wall and flow are obtained using previous studies. The achievements of this study can help the researchers by providing more detailed information about aortic aneurysm with intraluminal thrombus.

## Methods

### Geometry and material

The simplified geometry based on the geometry in,[18] which was applied to simulate abdominal aortic aneurysm is shown in Fig. 1. A two-dimensional axisymmetric model of stented three-layered aneurysm with ILT was constructed. The radii of inlet and outlet are the same and set to 12 mm and the maximum aneurysm radius was set to 30 mm. The thickness of the entire wall was chosen to be 2 mm and the thicknesses of the intima, media, and adventitia in aneurysm models were $t_i = 0.2$ mm, $t_m = 1.2$ mm, and $t_a = 0.6$ mm, respectively.[19] The vessel walls were modeled as a two-dimensional axisymmetric structure.

The stent wire diameter is 1 mm and has a total length of 90 mm and 10 braids. The center of stent was chosen to lie on the center of the aneurysm and the stent is assumed to be rigid and fixed.[20]

Blood was assumed to be Newtonian with a density of $\rho_f = 1050 \text{ kg/m}^3$ and a dynamic viscosity of $\mu = 0.0035$ Pa.s and treats as laminar flow.[2,21–23] The aneurysm wall was assumed to be an isotropic, linear, and elastic solid with a density of $\rho_s = 2000 \text{ kg/m}^3$, a Poisson's ratio $\eta = 0.45$, and mean Young's modulus E = 4.0 MPa. Young's modulus values of the intima, media, and adventitia are 1.6, 4.8, and 3.2 MPa, respectively.[24–27]

## Equation

The flow was assumed to be laminar Newtonian, viscous and incompressible.[28–30] The Navier–Stokes equations in Arbitrary Lagrangian-Eulerian (ALE) formulation are given in Equation (1).[23,26,31]

$$\rho_f \frac{\partial u}{\partial t} - \nabla \left[ \left( -p \right) I + \mu (\nabla u + (\nabla u)^T) \right] + \rho_f ((u - u_m)\nabla)u = F$$
$$\nabla u = 0$$

(1)

where $\rho_f$ is the fluid's density, u is the velocity field of the flow, p is the fluid pressure, I is the identity tensor, F is the volume force affecting the fluid, $u_m$ is the mesh veloci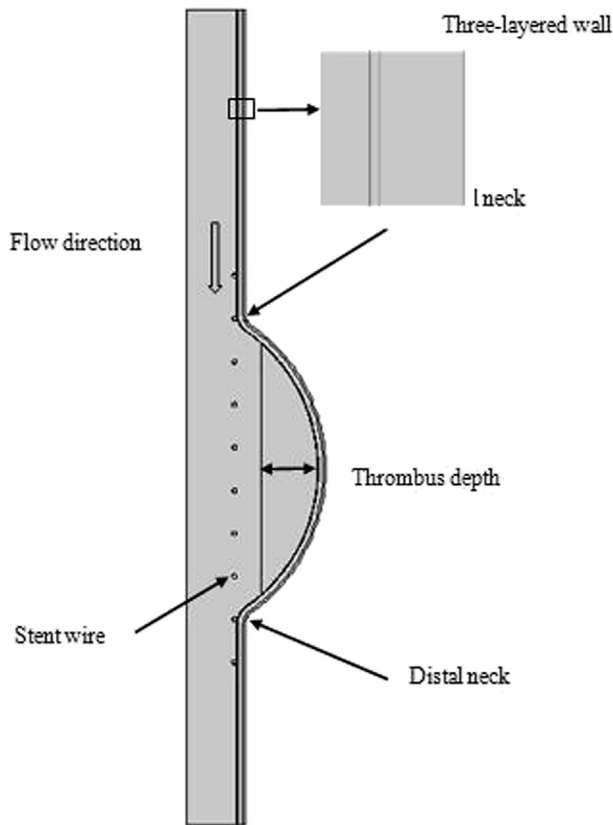ty due to the movement of the coordinate system, and r is the differential operator with respect to the Eulerian coordinate.[32] It is assumed that no gravitation or other volume forces affect the fluid, so F = 0. The structure deformations are solved using an elastic formulation. The governing equation for the solid can be described by Equation (2):[33]

$$\nabla \sigma + F_s = -\rho_s \frac{\partial^2 d_s}{\partial t^2}$$

(2)

where $\rho_s$ is the solid density, $\sigma$ is the Cauchy stress tensor, $F_s$ is the body force per unit volume, and $d_s$ is the displacement of the solid. The applied load from the fluid to the wall is given by Equation (3):[34]

$$F_T = -n\left( -pI + \eta \left( \nabla u + (\nabla u)^T \right) \right)$$

(3)

where n is the normal vector to the boundary. This load shows a sum of pressure and viscous forces.

## Boundary conditions

A time-dependent flow was applied at the inlet and a pressure boundary was assigned at the outlet of aorta in Figs. 2 and 3.[35] For the composite structure, the boundary conditions include fixed displacements at the inlet and the outlet, and free displacement of the wall. It should be noted that the composite layers are adhered and have no relative motion to each other. The stent is assumed to be rigid. This study is divided in two sections. In our first analysis the entire cavity is filled with thrombus in order to investigate the effect of change in modulus of elasticity on wall stress. Our second analysis includes nine subsequent sections with increasing intraluminal thrombus area by 10 percent until thrombus filled the entire cavity.

Simulation was performed using fully coupled fluid-structure interaction solving capability of commercial software COMSOL (United States VER 4.3b). For the solid and fluid model, four pulsatile cycle were computed, number of iteration per cycle and iteration tolerance is set to 1000 (each step equals to 0.001) and 0.001, respectively.
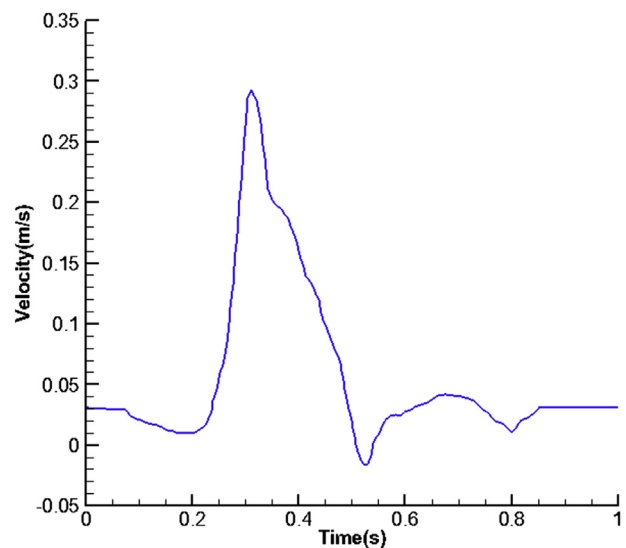


**Figure 1** Two-dimensional axisymmetric aneurysm model with thrombus and three layered wall.



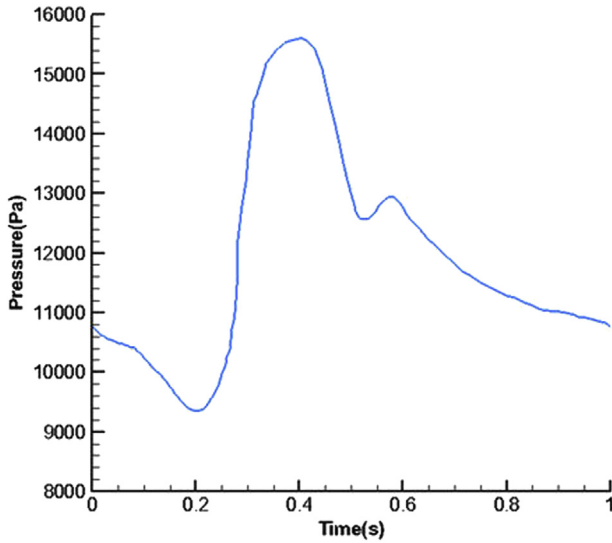**Figure 2** Flow waveform at the inlet of aorta.

**Figure 3**   Pressure wave form at the outlet.

To reach more accurate results, one common method is mesh refining until a convergent solution is obtained. With small elements the resultant computations converge to a stable value. In this case, we say that the problem has reached to the mesh independency. By shrinking the lattice with smaller elements, the accuracy of answers is not significantly changed, but we have more calculations. Therefore, the problem was solved for six times by mesh refining and our result converged and had no considerable change after step 4.

## Results

Figure 4 shows the flow volume rate for the inlet and outlet in the stented aneurysm model. It is expressed by:
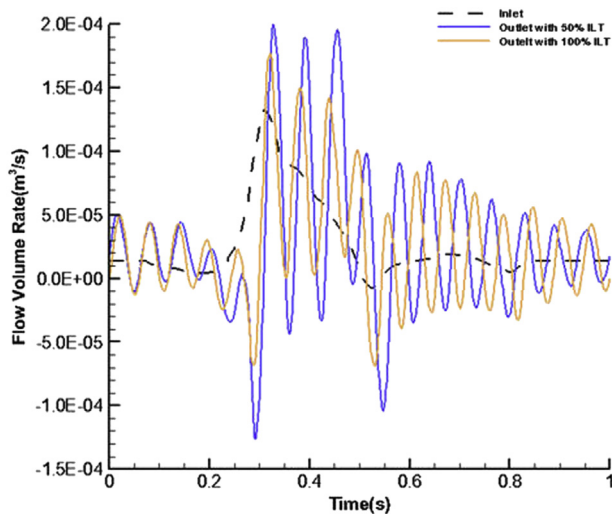


**Figure 4**   Temporal flow volume rate at the inlet and outlet for stented aneurysm with 50% and 100% of thrombus depth.

$$Q = \iint\limits_A v \, dA \qquad (4)$$

where V is the flow velocity and A is the cross-sectional area of the aorta. During one cycle, the flow volume passing through the outlet is the same as the flow volume passing through the inlet. This indicates that conservation of mass in the fluid flow is satisfied.

The contours of pressure change in fluid domain for six different values of intraluminal thrombus elasticity modulus in case of filled cavity at the time of peak pressure have been depicted in Fig. 5. Modulus of elasticity of thrombus was increased with the values of 0.1, 0.15, 0.2, 0.5,1, 2 MPa for parts a, b, c, d, e, f, respectively.

The blood flow velocity contours for the stented aneurysm model with different aforementioned intraluminal thrombus elastic modulus at the time of peak flow, have been illustrated in Fig. 6. As shown in part (a), because of lower elastic modulus and higher displacement for the thrombus compared to those of intima, the blood flow velocity is decreased as we move from the inlet to the outlet due to increase in cross-sectional area at the thrombus region.

Figure 7 shows pressure contours for the different thrombus depth percentage increased from 10% to 100% with the elastic modulus of 0.2 MPa at the time of peak pressure.[36] Although there is no notable considerable difference between the pressure values at the upstream before reaching to the thrombus region for all cases (10%—100% thrombus depth), an increase takes place in pressure values at the downstream after thrombus region particularly from 80% to 100% thrombus depth. It can be concluded that the increase in thrombus depth even approximately up to 50% has not significant effect on pressure change. The effect of thrombus on pressure may be dominant from 50% to 100% depth.

Figure 8 shows velocity contours for stented aneurysm model with different thrombus depth that varies from 10% to 100% at the time of peak flow when $E_{th} = 0.2$ MPa. At the entrance of the aneurysm, the blood flow velocity is much higher than that of downstream.

Figures 9 and 10 present the von Mises stress distribution along the wall thickness at the inflection points when entire cavity of aneurysm is filled with thrombus at the time peak flow and peak pressure, respectively.

Figures 11 and 12 show von Mises stress distribution along the wall thickness as the thrombus depth with the elastic modulus of 0.2 MPa fills 10%—100% of the entire cavity at the time of peak flow and peak pressure, respectively.

## Discussion

According to the Fig. 5a, the blood pressure increases with moving from the inlet toward to the outlet. This is because the thrombus has the lower modulus of elasticity and consequently higher displacement than the intima. Therefore, the cross-sectional area of the vessel increases at the proximal neck of thrombus which makes the blood flow velocity to be decreased which in turn causes the blood pressure to be increased. As the modulus of elasticity of
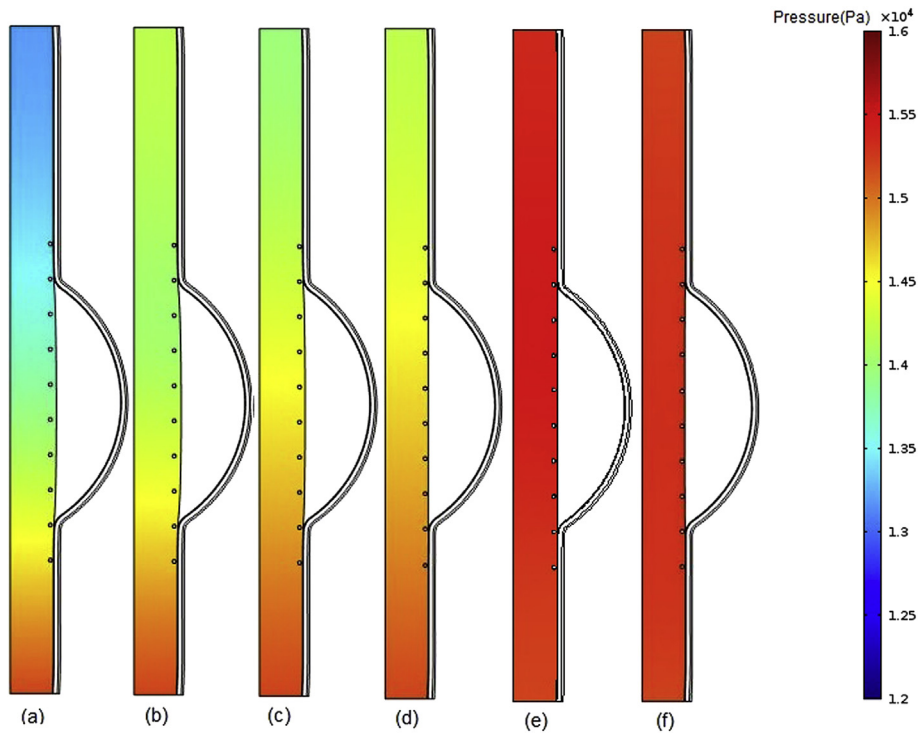
**Figure 5** Comparison of pressure in stented aneurysm model in the case of filled cavity with ILT and changing thrombus modulus of elasticity ($E_{th}$) at the time of peak pressure for a) $E_{th} = 0.1$ MPa, b) $E_{th} = 0.15$ MPa, c) $E_{th} = 0.2$ MPa, d) $E_{th} = 0.5$ MPa, e) $E_{th} = 1$ MPa, f) $E_{th} = 2$ MPa.

thrombus increases, the difference between pressure values of the inlet and outlet decreases. Since the difference between elasticity modulus of thrombus and intima has the minimum value in part (e), the lowest pressure

change occurs in this part but in general the pressure magnitude has been increased and is about that of normal person,[37] in comparison with previous parts of Fig. 5. As appeared in part (f), the pressure magnitude is lower than
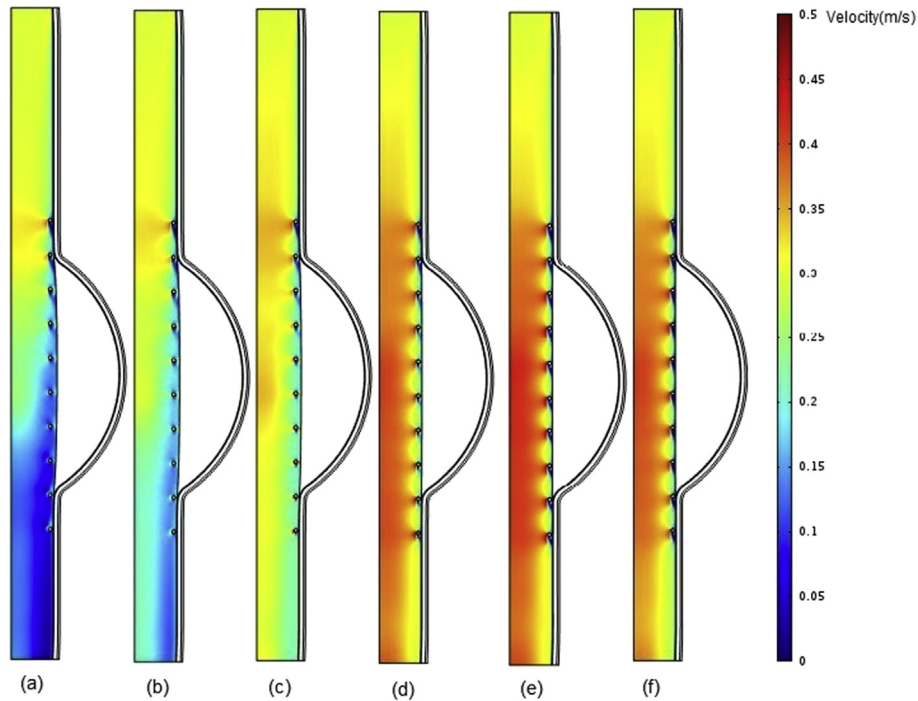


**Figure 6** Comparison of pressure in stented aneurysm model in the case of filled cavity with ILT and changing thrombus modulus of elasticity ($E_{th}$) at the time of peak flow for a) $E_{th} = 0.1$ MPa b) $E_{th} = 0.15$ MPa, c) $E_{th} = 0.2$ MPa, d) $E_{th} = 0.5$ MPa, e) $E_{th} = 1$ MPa, and f) $E_{th} = 2$ MPa.
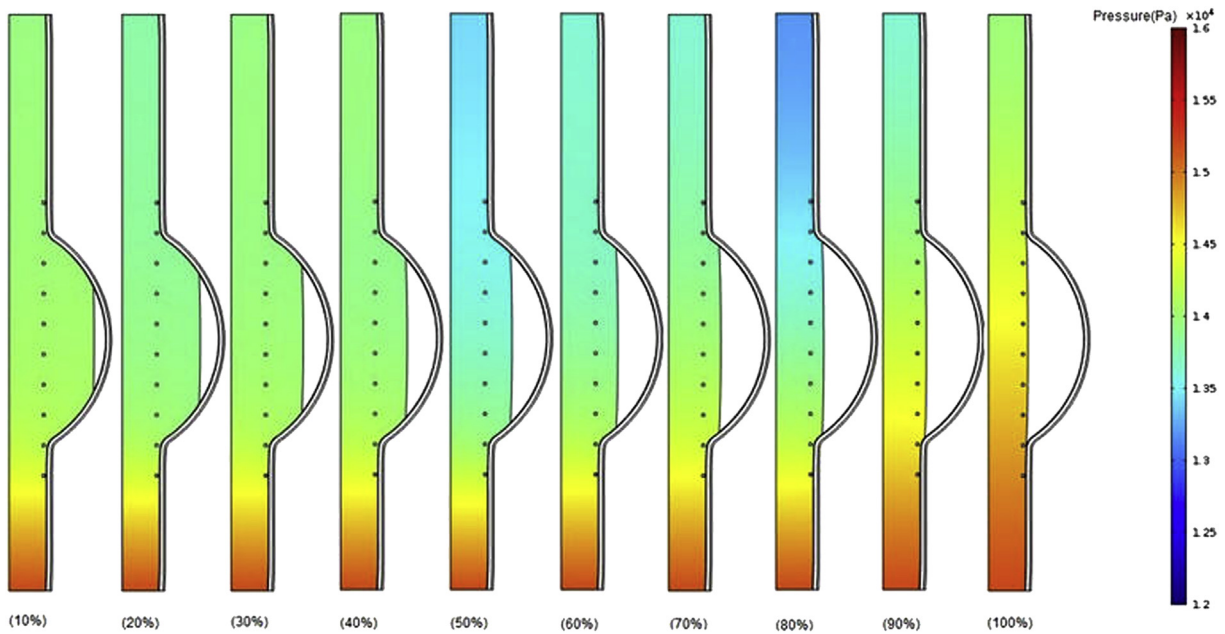
**Figure 7** Comparison of pressure in the case of changing thrombus depth grows from 10% to 100% of aneurysm cavity with constant thrombus modulus of elasticity ($E_{th}$ = 0.2 MPa) at the time of peak pressure.

that of part (e). This may be due to a higher thrombus elastic modulus compared to that of the intima, which makes the blood to be uniformly.

It can be understood from the blood flow velocity contours (Fig. 6.) that the increase in thrombus elastic modulus causes the blood flow velocity to be increased. This is due to decrease in thrombus wall displacement. It is worth mentioned to say blood flow velocity for part (f), is lower than that of part (e). It may conclude that the highest

velocity is obtained in the presence of uniform modulus of elasticity along the vessel.

The thrombus depth can affect the change in pressure if the thrombus depth is approximately more than 50% of cavity. Furthermore, it can be seen that the velocity increases by the growth of thrombus depth and this may be due to reduction in cross-sectional area at the distal neck.

At the time peak flow and peak pressure with the cavity-filled thrombus the media layer has the highest stress among three layers. Furthermore, the wall stress decreases
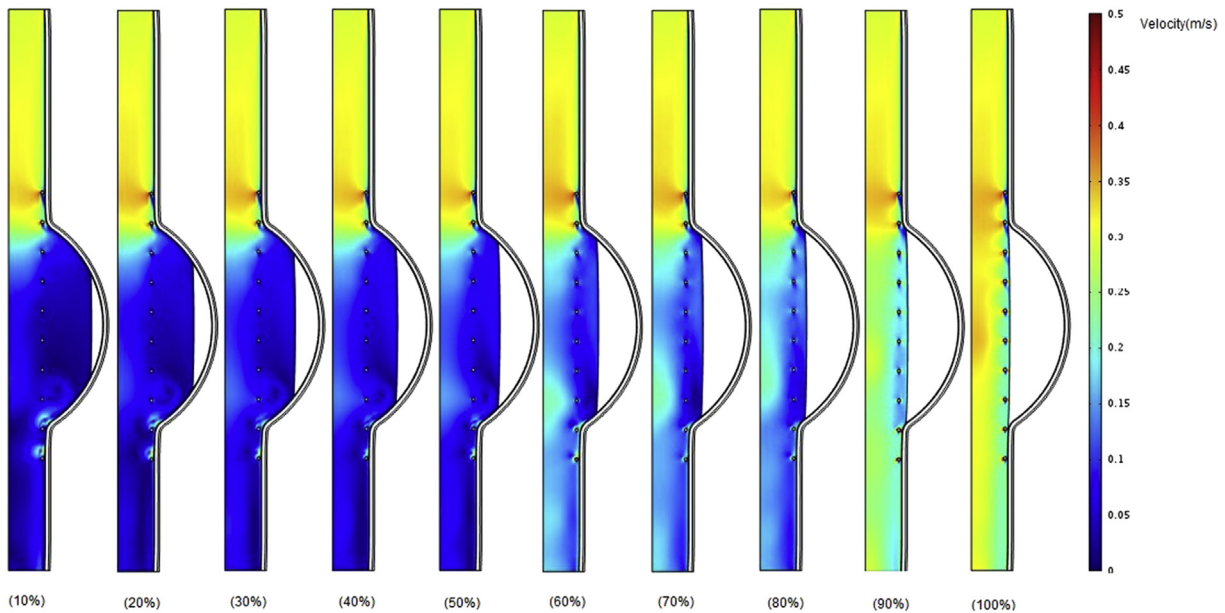


**Figure 8** Comparison of velocity in the case of changing thrombus depth grows from 10% to 100% of aneurysm cavity with constant thrombus modulus of elasticity ($E_{th}$ = 0.2 MPa) at the time of peak flow.
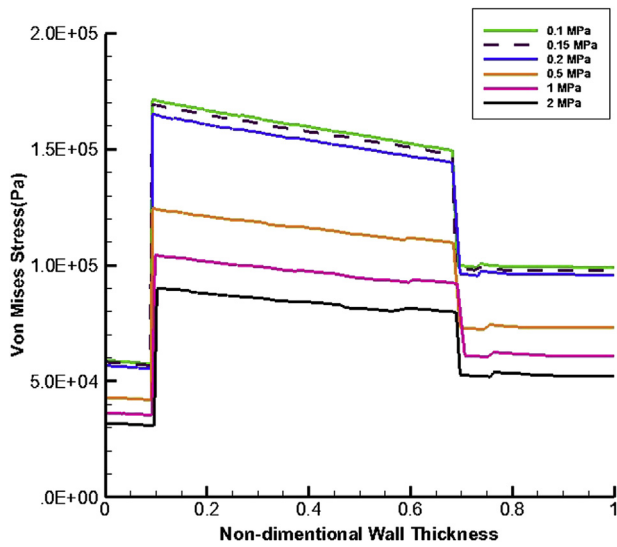
**Figure 9** von Mises stress distribution along the wall thickness at the inflection points in the case of filled aneurysm cavity with thrombus at the time of peak flow.

by the value of 46% at the time of peak flow and 38% at the time of peak pressure as the elastic modulus of thrombus increases from 0.1 to 2 MPa. By increasing thrombus depth the wall stress is reduced. This reduction is considerable when the thrombus depth is higher than 60%. moreover, the wall stress decreases by the value of 27% at the time of peak flow and 22% at the time of peak pressure as thrombus depth grows from 10% to 100%.

## Conclusion

The purpose of present study was to investigate hemodynamic parameters like blood flow velocity, pressure and
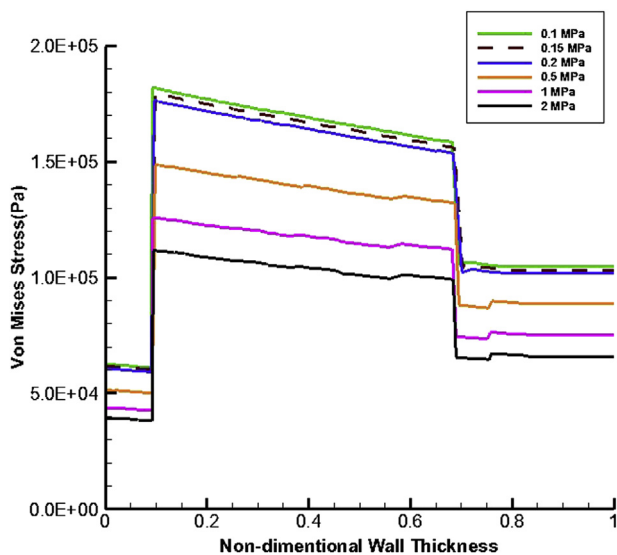


**Figure 10** von Mises stress distribution along the wall thickness at the inflection points in the case of filled aneurysm cavity with thrombus at the time of peak pressure.
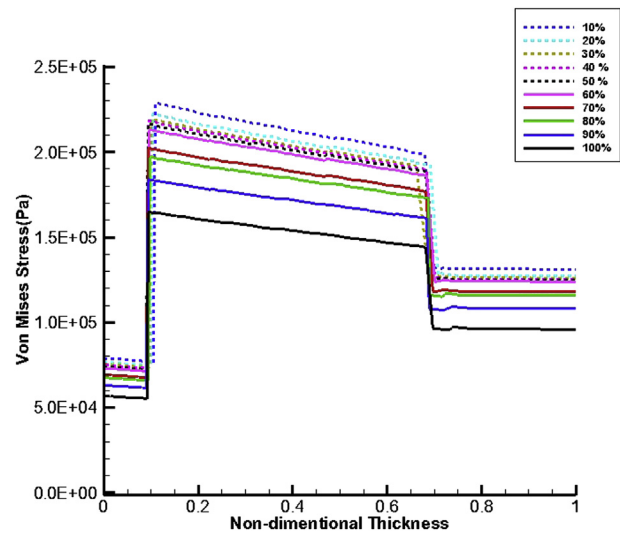


**Figure 11** von Mises stress distribution along the wall thickness at the inflection points when thrombus depth grows from 10% to 100% of aneurysm cavity and elastic modulus of thrombus is constant ($E_{th} = 0.2$ MPa) at the time of peak flow.

wall stress distribution through a stented aortic aneurysm with intraluminal thrombus. A two-dimensional axisymmetric model of aortic aneurysm with various both depth and elastic modulus of thrombus in the presence of pulsatile flow with considering fluid-solid interaction was simulated. The results revealed that the wall stress decreases by the growth of thrombus elastic modulus for both times of peak flow and peak pressure and the difference between pressure values of the inlet and outlet at the time of peak pressure decreases in the case of reduction in difference between elastic modulus of intima and thrombus.
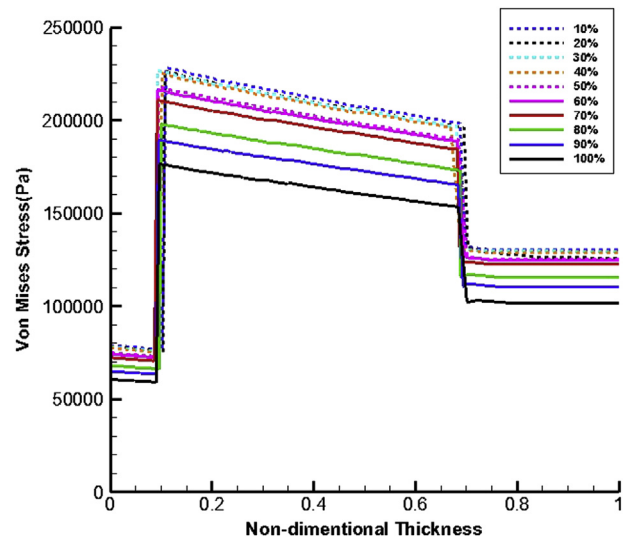


**Figure 12** von Mises stress distribution along the wall thickness at the inflection points when thrombus depth grows from 10% to 100% of aneurysm cavity and elastic modulus of thrombus is constant ($E_{th} = 0.2$ MPa) at the time of peak pressure.

Furthermore, at the time of peak flow as the thrombus elastic modulus closes to that of intima, the blood flow velocity increases. The amount of thrombus depth has significant effect on wall stress at both times of peak flow and peak pressure in such a way by increase in thrombus depth, the wall stress can be decreased and when thrombus depth is approximately higher than 50% of entire cavity, the pressure and velocity increases at the peak pressure and velocity times, respectively. Our results also show that the media layer is subjected to higher loads than other layers and that the stresses are much higher in the media layer in all cases. The achievements of this study can help the researchers by providing more detailed information about aortic aneurysm with intraluminal thrombus.

## Conflicts of interest

We declare that we have no conflicts of interest.

## Acknowledgments

## References

1. Abdi M, Karimi A, Navidbakhsh M, Hassani K, Faghihi S. Modeling of cerebral aneurysm using equivalent electrical circuit (Lumped Model). *Perfusion* 2014;**29**(2):142—52.
2. Abdi M, Karimi A, Navidbakhsh M, Pirzad Jahromi G, Hassani K. A lumped parameter mathematical model to analyze the effects of tachycardia and bradycardia on the cardiovascular system. *Int J Numer Model* 2014. http://dx.doi.org/10.1002/jnm.2010.
3. Abdi M, Karimi A, Navidbakhsh M, Rahmati M, Hassani K. Modeling of coronary artery balloon-angioplasty using equivalent electrical circuit. *Biomed Eng — Appl Basis Commun* 2013; **26**(3):1450039—49.
4. Vorp DA. Biomechanics of abdominal aortic aneurysm. *J Biomech* 2007;**40**(9):1887—902.
5. Wilson JS, Virag L, Di Achille P, Karšaj I, Humphrey JD. Biochemomechanics of intraluminal thrombus in abdominal aortic aneurysms. *J Biomech Eng* 2013;**135**(2):021011.
6. Karimi A, Navidbakhsh M. A comparative study on the uniaxial mechanical properties of the umbilical vein and umbilical artery using different stress—strain definitions. *Australas Phys Eng Sci Med* 2014. http://dx.doi.org/10.1007/s13246-014-0294-5.
7. Karimi A, Navidbakhsh M, Shojaei A, Hassani K, Faghihi S. Study of plaque vulnerability in coronary artery using Mooney—Rivlin model: a combination of finite element and experimental method. *Biomed Eng — Appl Basis Commun* 2014;**26**(1): 1450013—20.
8. Karimi A, Navidbakhsh M, Rezaee T, Hassani K. Measurement of the circumferential mechanical properties of the umbilical vein: experimental and numerical analyses. *Comput Methods Biomech Biomed Eng* 2014. http://dx.doi.org/10.1080/10255842.2014.910513.
9. Karimi A, Navidbakhsh M, Shojaei A, Faghihi S. Measurement of the uniaxial mechanical properties of healthy and atherosclerotic human coronary arteries. *Mater Sci Eng C* 2013;**33**(5): 2550—4.
10. Humphrey J, Taylor C. Intracranial and abdominal aortic aneurysms: similarities, differences, and need for a new class of computational models. *Annu Rev Biomed Eng* 2008;**10**:221.
11. Canham PB. The minimum energy of bending as a possible explanation of the biconcave shape of the human red blood cell. *J Theor Biol* 1970;**26**(1):61—81.
12. Chuter T, Ivancev K, Malina M, et al. Aneurysm pressure following endovascular exclusion. *Eur J Vasc Endovasc Surg* 1997;**13**(1):85—7.
13. Di Martino ES, Bohra A, Scotti C, Finol E, Vorp DA. Wall stresses before and after endovascular repair of abdominal aortic aneurysms. ASME 2004 International Mechanical Engineering Congress and Exposition. *Am Soc Mech Eng* 2004;**2004**:325—6.
14. Lieber BB, Livescu V, Hopkins L, Wakhloo AK. Particle image velocimetry assessment of stent design influence on intra-aneurysmal flow. *Ann Biomed Eng* 2002;**30**(6):768—77.
15. Caves JM, Cui W, Wen J, Kumar VA, Haller CA, Chaikof EL. Elastin-like protein matrix reinforced with collagen microfibers for soft tissue repair. *Biomaterials* 2011;**32**(23):5371—9.
16. Mower WR, Baraff LJ, Sneyd J. Stress distributions in vascular aneurysms: factors affecting risk of aneurysm rupture. *J Surg Res* 1993;**55**(2):155—61.
17. Sun Z, Chaichana T. Investigation of the hemodynamic effect of stent wires on renal arteries in patients with abdominal aortic aneurysms treated with suprarenal stent-grafts. *Cardiovasc Interv Radiol* 2009;**32**(4):647—57.
18. Gao F, Watanabe M, Matsuzawa T. Stress analysis in a layered aortic arch model under pulsatile blood flow. *Biomed Eng Online* 2006;**5**(25):1—11.
19. Choi HS, Vito R. Two-dimensional stress-strain relationship for canine pericardium. *J Biomech Eng* 1990;**112**(2):153—9.
20. Gao F, Tang D, Guo Z, Sakamoto M, Matsuzawa T. Stress analysis in layered aortic arch model: influence of arch aneurysm and wall stiffness. *ICCES — Int Conf Comput Exp Eng Sci* 2007; **2007**:21—8.
21. Gao F, Ueda H, Gang L, Okada H. Fluid structure interaction simulation in three-layered aortic aneurysm model under pulsatile flow: comparison of wrapping and stenting. *J Biomech* 2013;**46**(7):1335—42.
22. Gao F, Guo Z, Sakamoto M, Matsuzawa T. Fluid-structure interaction within a layered aortic arch model. *J Biol Phys* 2006;**32**(5):435—54.
23. Karimi A, Navidbakhsh M, Yamada H, Razaghi R. A nonlinear finite element simulation of balloon expandable stent for assessment of plaque vulnerability inside a stenotic artery. *Med Biol Eng Comput* 2014;**52**(5):589—99.
24. Karimi A, Navidbakhsh M, Razaghi R. A finite element study of balloon expandable stent for plaque and arterial wall vulnerability assessment. *J Appl Phys* 2014;**116**(5):044701—10.
25. Karimi A, Navidbakhsh M, Razaghi R. Plaque and arterial vulnerability investigation in a three-layer atherosclerotic human coronary artery using computational fluid-structure interaction method. *J Appl Phys* 2014;**116**(9):064701—10.
26. Karimi A, Navidbakhsh M, Razaghi R, Haghpanahi M. A computational fluid-structure interaction model for plaque vulnerability assessment in atherosclerotic human coronary arteries. *J Appl Phys* 2014;**115**(14):144702—11.
27. Abdi M, Karimi A. A computational electrical analogy model to evaluate the effect of internal carotid artery stenosis on circle of willis efferent arteries pressure. *J Biomater Tissue Eng* 2014;**4**(9):749—54.
28. Karimi A, Navidbakhsh M, Alizadeh M, Shojaei A. A comparative study on the mechanical properties of the umbilical vein and umbilical artery under uniaxial loading. *Artery Res* 2014;**8**(2): 51—6.
29. Karimi A, Navidbakhsh M, Haghighatnama M, Motevalli Haghi A. Determination of the axial and circumferential mechanical properties of the skin tissue using experimental testing and

constitutive modeling. *Comput Methods Biomech Biomed Eng* 2014. http://dx.doi.org/10.1080/10255842.2014.961441.

30. Karimi A, Navidbakhsh M, Faghihi S, Shojaei A, Hassani K. A finite element investigation on plaque vulnerability in realistic healthy and atherosclerotic human coronary arteries. *Proc I Mech Part H* 2013;**227**(2):148—61.

31. Taylor CA, Figueroa C. Patient-specific modeling of cardiovascular mechanics. *Annu Rev Biomed Eng* 2009;**11**:109—34.

32. Mills CJ, Gabe IT, Gault JH, Mason DT, Ross Jr J, Braunwald E, et al. Pressure-flow relationships and vascular impedance in man. *Cardiovasc Res* 1970;**4**(4):405—17.

33. Mower WR, Quiñones WJ, Gambhir SS. Effect of intraluminal thrombus on abdominal aortic aneurysm wall stress. *J Vasc Surg* 1997;**26**(4):602—8.

34. Le Tallec P, Mouro J. Fluid structure interaction with large structural displacements. *Comput Methods Appl Mech Eng* 2001;**190**(24):3039—67.

35. Liu WK, Chang H. Efficient computational procedures for long-time duration fluid-structure interaction problems. *J Press Vessel Tech* 1984;**106**(4):317—22.

36. Daly C, Odland G. Age-related changes in the mechanical properties of human skin. J Investig Dermatol 9009;73(1): 84—87.

37. Cooke TDV, Sled EA, Scudamore RA. Frontal plane knee alignment: a call for standardized measurement. *J Rheumatol* 2007;**34**(9):1796.